Chapter5
Simulation Results

In this chapter, we demonstrate performances of the synchronization schemes for Eureka 147 DAB, DVB-T and IEEE 802.16a. In this thesis, the sample clocks of the users and the base station are assumed to be identical.

5.1 Eureka 147 DAB System

5.1.1 Simulation Parameters and Channel Conditions

In this section, we will present the simulation results of our proposed synchronization scheme for Eureka 147 DAB system. As for the environment, an AWGN channel and multipath channel are assumed. We also assume mode-III OFDM signaling is used in the Eureka 147 DAB system for the simulation, because mode-III has the shortest symbol time and the fewest pilot data that makes the synchronization task more challenging. We choose the “Vehicular B” channel parameters defined by

ETSI. The multipath time delays and the averaged power of the multipath gains of the "Vehicular B" channel are shown in Table 5.2.

Table 5.1 System parameter of mode-III Eureka 147 DAB

Parameter	Mode III
Total number of carriers	256
Number of used carriers	196
Carrier spacing	8 KHz
Sampling frequency	2.048 MHz
OFDM symbol time	156 μs
Useful time	125 μs
Cyclic prefix time	31 μs
Null symbol duration	168 μs (345 samples)

Table 5.2 ETSI "Vehicular B" channel model

Tap	Time delays (μs)	Average Power	
		(dB)	(normalized)
1	0	-2.5	0.32
2	0.3	0	0.575
3	8.9	-12.8	0.029
4	12.9	-10.0	0.058
5	17.1	-25.2	0.002
6	20	-16.0	0.014

5.1.2 Performance of Frame Detection

Performance of the frame detection synchronization algorithm was evaluated in the multipath channel. The frame detection error rate is shown as a function of SNR in Figure 5.1. The threshold is set to 2 which makes the scheme could work under 0dB. Since the miss probability was down to 10^{-4} when SNR 3dB, it would appear that the frame detection algorithm can achieve a good performance under the multipath

channel.

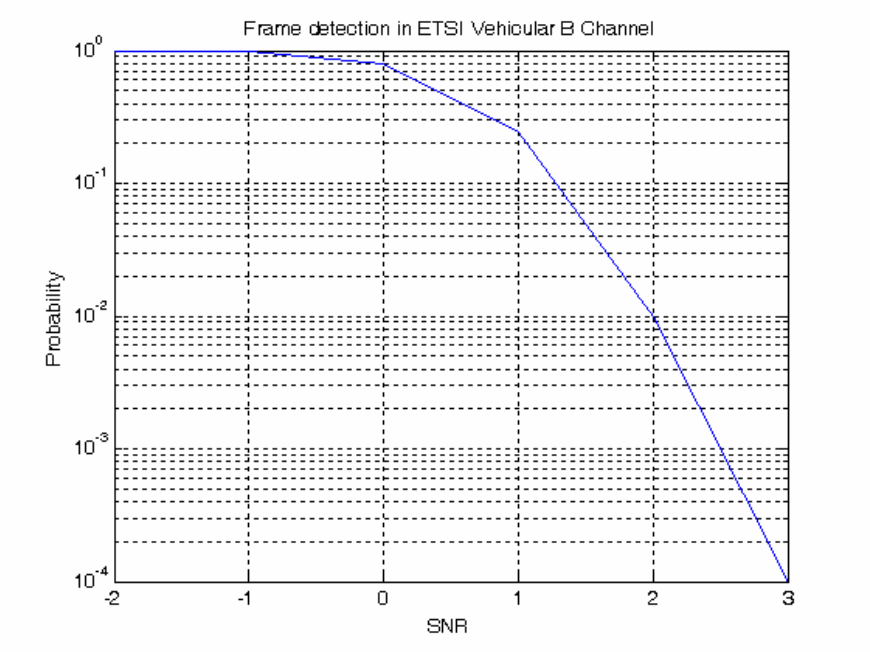

Figure 5.1 Performances of the mode-III frame synchronization

5.1.3 Performance of Symbol Timing and Fractional Frequency Synchronization

Figure 5.2(a) shows the standard deviation of the symbol timing estimation scheme as a function of SNR in AWGN channel. As long as the symbol time is in the guard interval, there is no BER degradation, as compared with the perfect symbol timing estimation. Figure 5.2(b) shows the standard deviation of the symbol timing estimation scheme in the assumed multipath channel. The synchronization performance under the multipath channel is poorer than that of AWGN channel. From these simulations, the conventional method that only adopts the correlation part has the enough performance, because the timing error is small enough to be kept in the cyclic prefix region and both ISI and ICI will not occur. For this reason, the conventional method is chosen in our work.

We use the conventional method and ML estimation to simulate the fractional

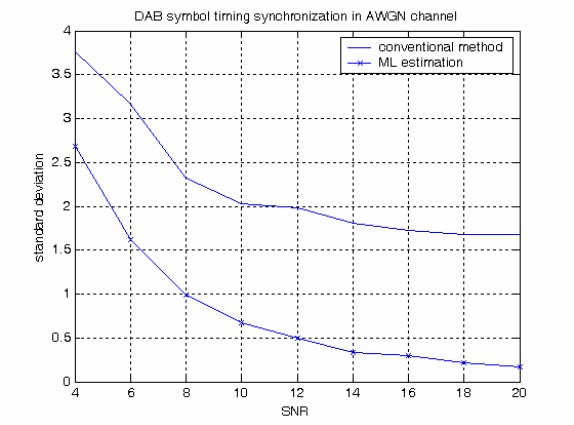

(a)

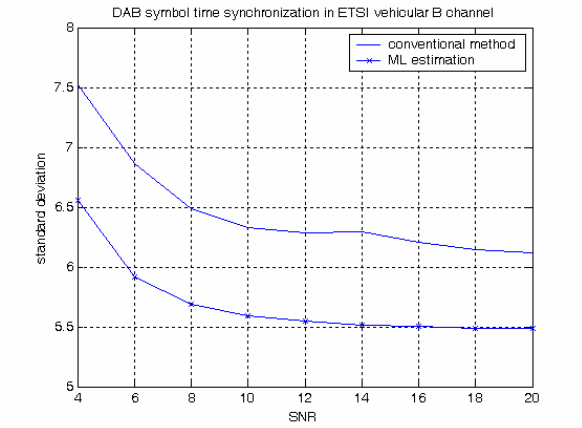

(b)

Figure 5.2 The standard deviations of symbol timing synchronization vs. SNR (a) in AWGN channel (b) in the ETSI ”Vehicular B” multipath channel, of DAB system.

frequency offset. It can be observed from Figure 5.3 that the FFO estimation algorithm has the same detection ability under different initial FFO’s which are smaller than 0.5 carrier spacing. Thus, we only choose the case of initial offset of 0.2 carrier spacing to simulate its performance. Figure 5.4 shows the standard deviation when the carrier frequency offset is 0.2 subcarrier spacing in multipath channel.

Performances of the two fractional frequency estimations are almost the same for a small range from the symbol start location. It can be observed from Figure 5.4 that the conventional method achieves a standard deviation less than 0.05 subcarrier spacing in the multipath channel even when SNR is below 4dB.

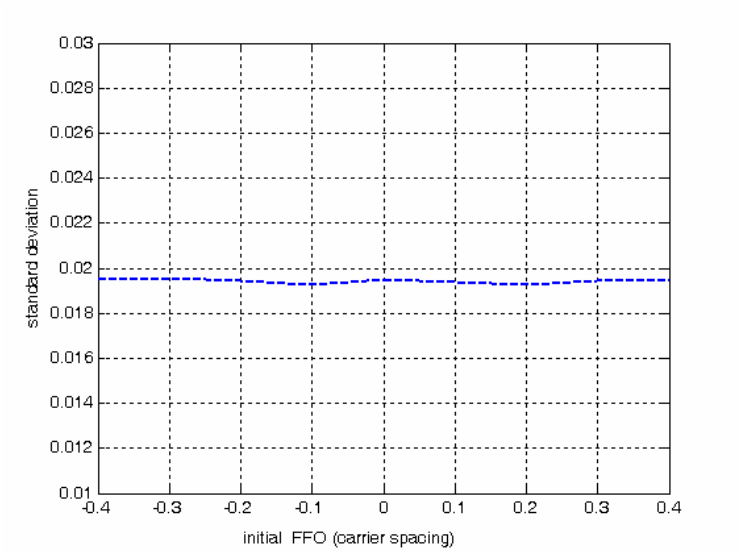

Figure 5.3 Standard deviations of FFO synchronization versus different initial FFO's with SNR 9dB in AWGN channel.

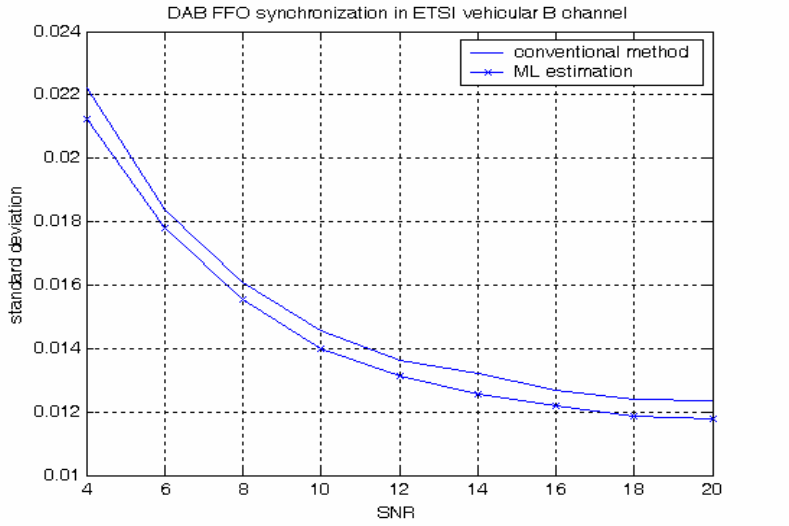

Figure 5.4 Standard deviations of fractional frequency offset synchronization versus SNR in ETSI "Vehicular B" multipath channel, of DAB system, FFO=0.2.

5.1.4 Performance of the Integral Frequency Synchronization

Figure 5.5 shows our proposed four integral frequency synchronization methods in multipath channel. It is observed that Method 4 has better performance than the others, because it is more robust against multipath channel. However, Method1 has the lowest complexity of all.

Method1: $D_1(i) = \left| \sum_k R_{k+i} C_k^* R_{k+1+i}^* \right|$.

Method2: $D_2(i) = \dfrac{\left| \sum_k R_{k+i} C_k^* R_{k+1+i}^* \right|^2}{(\sum_k |R_{k+i}|^2)^2}$.

Method3: $D_3(i) = \dfrac{\left| \sum_k R_{k+i} C_k^* R_{k+1+i}^* \right|^2}{(\sum_k |R_{k+1+i}|^2)^2}$

Method4: $D_4(i) = \dfrac{\left| \sum_k R_{k+i} C_k^* R_{k+1+i}^* \right|^2}{(0.5*(\sum_k |R_{k+i}|^2 + \sum_k |R_{k+1+i}|^2))^2}$

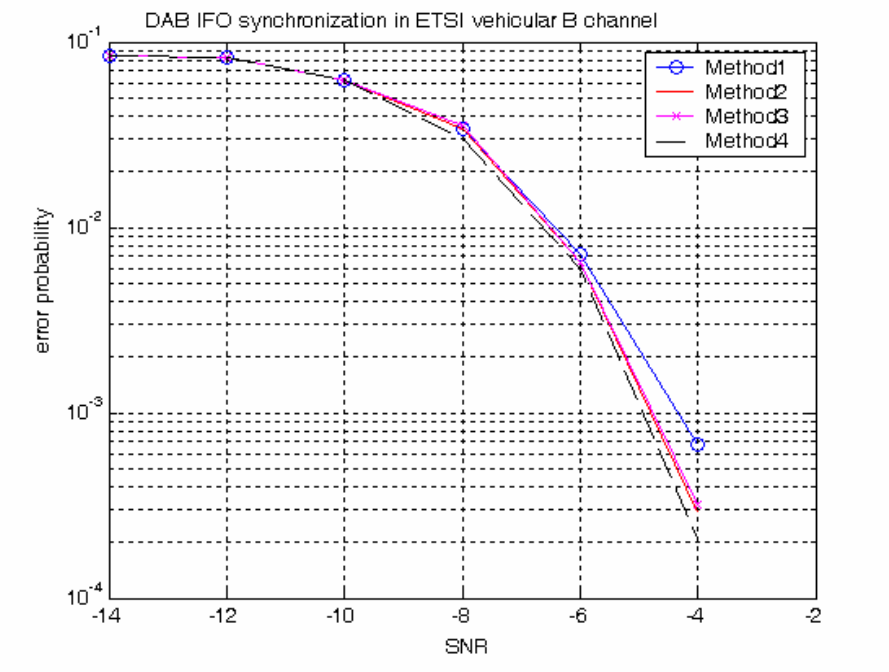

Figure 5.5 Performances of integral frequency synchronization of four proposed methods in multipath channel, assuming perfect symbol timing synchronization, mode-III DVB, IFO=2 carrier spacings.

Figure 5.6 shows the performance comparison of the proposed Method1 and the conventional method in AWGN channel condition. We can find that the conventional matching algorithm has better performance than the proposed method, under the condition of perfect symbol timing synchronization. However, the estimated symbol locations are randomly distributed and not always exact in practice. Since an timing offset gives rise to a phase rotations of subcarriers, the conventional matched filter fail to estimate the symbol timing accurately. From Figure 5.7, our suggested Method1 is more robust against the symbol timing error. The Method1 is also reliable in the multipath channel as shown in Figure 5.8.

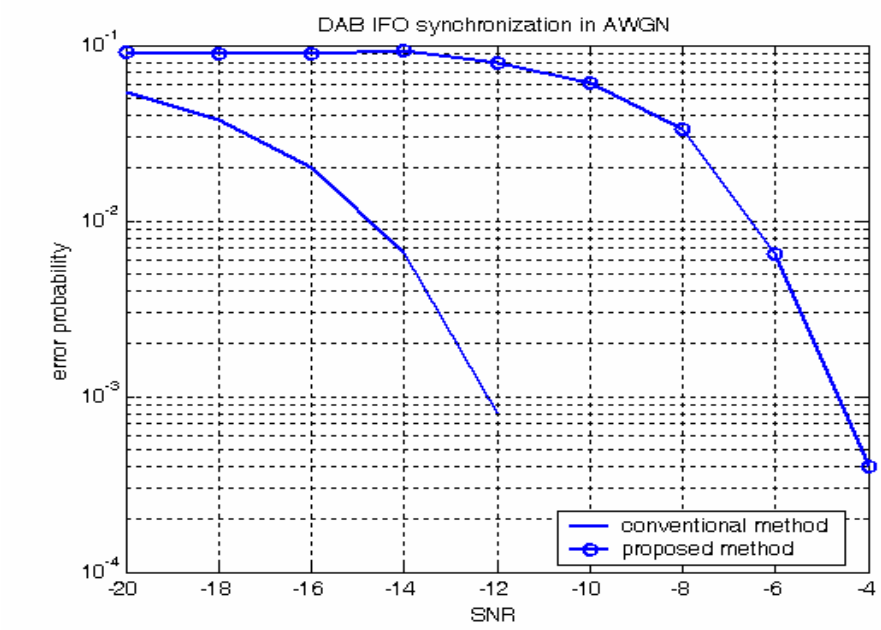

Figure 5.6 Performances of integral frequency synchronization of the conventional method and proposed Method1 in AWGN channel, assuming perfect symbol timing synchronization, mode-III DVB, IFO=2 carrier spacings.

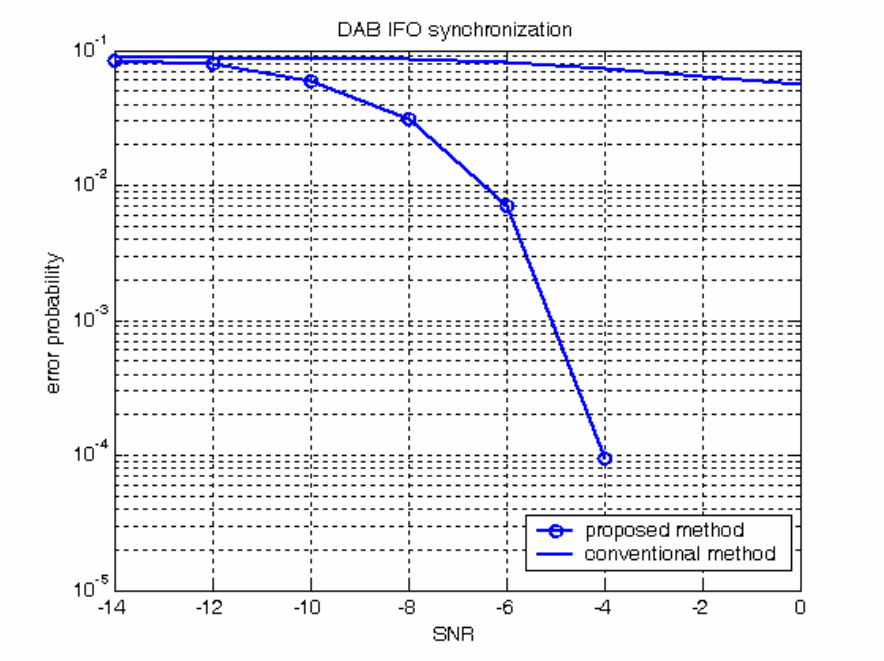

Figure 5.7 Performance of the conventional and proposed Method1 for IFO synchronization in AWGN channel, with 5-sample of symbol timing synchronization error, DAB mode-III, IFO=2 carrier spacings.

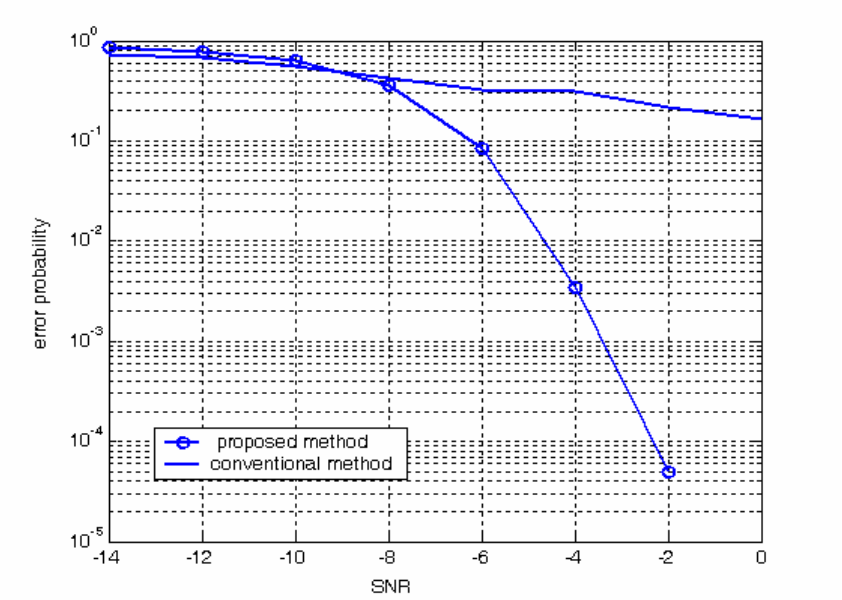

Figure 5.8 Performance of the conventional and proposed Method1 for IFO synchronization in the assumed multipath channel, with 5-sample of symbol timing synchronization error, DAB mode-III, IFO=2 carrier spacings.

5.1.5 Overall Performance

Overall BER performance of the combined proposed frame detection, symbol timing synchronization and frequency synchronization methods are shown in Figure 5.9, Figure 5.10 and Figure 5.11. Here the added initial frequency offset is 2.2 carrier spacings. Figure 5.11 shows the performance in a fading environment. Here we have $f_d T_S = 0.00624$, where f_d is the maximum Doppler shift frequency. From the figures, BER performance of our method approaches to the perfect synchronization case.

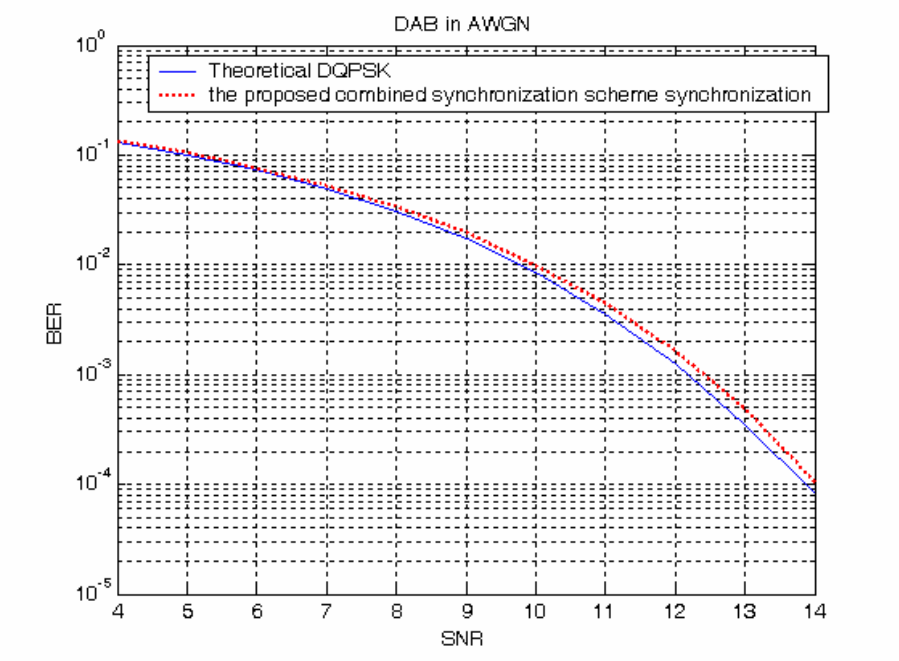

Figure 5.9 BER performances of the proposed combined synchronization scheme in AWGN channel, mode-III DAB system.

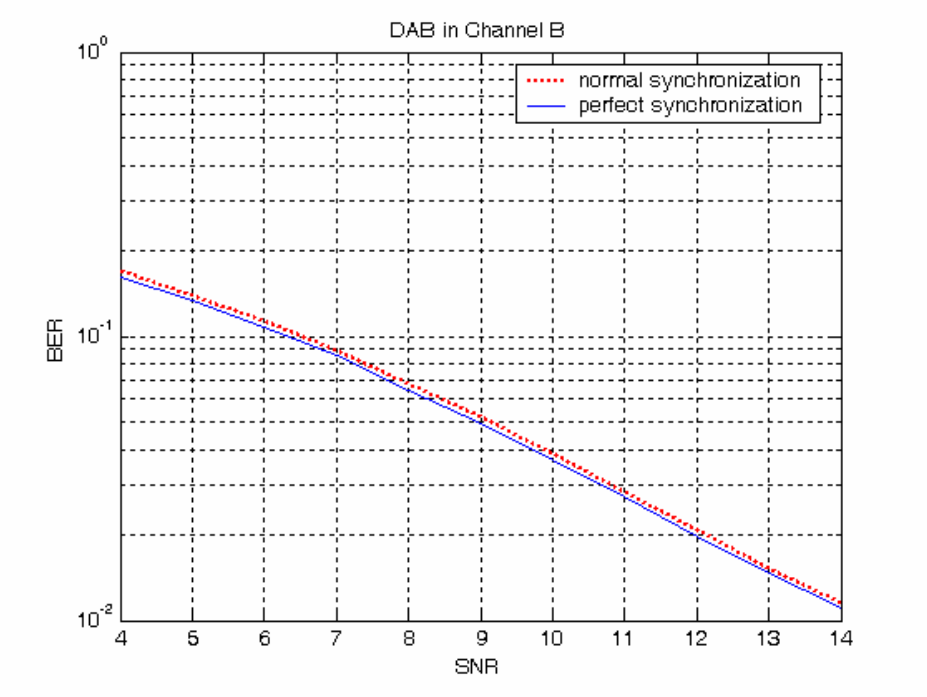

Figure 5.10 BER performances f the proposed combined synchronization scheme in ETSI “Vehicular B” Channel

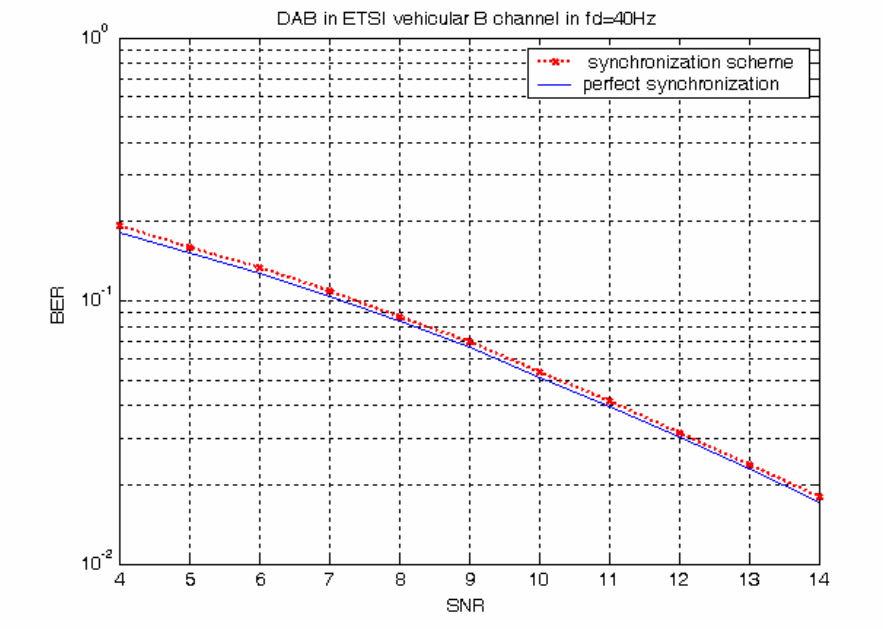

Figure 5.11 BER performances f the proposed combined synchronization scheme in ETSI “Vehicular B” Channel with $f_d T_s = 0.00624$.

5.2 DVB-T

5.2.1 Simulation and Parameters and Channel Environments

Performance of the system has been simulated in an AWGN channel and multipath channel [7]. The system parameters are listed in Table 5.3. The multipath channel model has been generated from the following equations, where $x(t)$ and $y(t)$ are transmitted and received signals related by:

$$y(t) = \frac{\rho_0 \cdot x(t) + \sum_{i=1}^{N} \rho_i e^{-j\theta_i} x(t-\tau_i)}{\sqrt{\sum_{i=0}^{N} \rho_i^2}} \tag{5.1}$$

$$\rho_0 = \sqrt{10 \sum_{i=1}^{N} \rho_i^{\,2}}$$

where N is the number of echoes equals to 20 , ρ_0 is the line-of-sight ray and θ_i, ρ_i, τ_i are the phase, attenuation, relative delay of the i-th path, respectively, which are listed in Table 5.4.

Table 5.3 System parameters of DVB-T 2K and 8K mode

Parameter	2K mode	8K mode
Number of the total carriers	2048	8192
Number of the used carriers	1705	6817
Carrier spacing	4464 Hz	1116 Hz
Sampling frequency	9.142 MHz	9.142 MHz
Effective bandwidth	7.61MHz	7.61MHz
Useful symbol time	224 μs	896 μs
Cyclic prefix time / Useful time	1/32 (64 samples)	1/32 (256 samples)

Table 5.4 Relative power, phase and delay values of DVB-T system

i	ρ_i	$\tau_i[\mu s]$	$\theta_i[rad]$
1	0,057 662	1,003 019	4,855 121
2	0,176 809	5,422 091	3,419 109
3	0,407 163	0,518 650	5,864 470
4	0,303 585	2,751 772	2,215 894
5	0,258 782	0,602 895	3,758 058
6	0,061 831	1,016 585	5,430 202
7	0,150 340	0,143 556	3,952 093
8	0,051 534	0,153 832	1,093 586
7	0,185 074	3,324 866	5,775 198
10	0,400 967	1,935 570	0,154 459
11	0,295 723	0,429 948	5,928 383
12	0,350 825	3,228 872	3,053 023
13	0,262 909	0,848 831	0,628 578
14	0,225 894	0,073 883	2,128 544
15	0,170 996	0,203 952	1,099 463
16	0,149 723	0,194 207	3,462 951
17	0,240 140	0,924 450	3,664 773
18	0,116 587	1,381 320	2,833 799
19	0,221 155	0,640 512	3,334 290
20	0,259 730	1,368 671	0,393 889

5.2.2 Performance of Symbol Timing and Fractional Frequency Synchronization

Figure 5.12(a) shows the standard deviations of those 3 symbol timing synchronization methods in 2K mode and AWGN channel. The conventional method that only adopts the correlated part has the worst performance of all. Its poor performance is because of the fact that the energy variations of the correlated samples are not compensated. Hence, it raises the error probability in symbol detection. For the simplified MLE method, the probability of time synchronization error is a little higher than that of ML estimation at low SNR because of using the suboptimal fixed

$\rho = 1$.

Error standard deviations of these three methods in the multipath channel condition are shown in Figure 5.12(b). We can find that error probability of the conventional symbol synchronization method is much higher than the other methods, because the channel length is almost equal to guard interval. The figure shows that the detection probability is low due to large standard deviations of the symbol synchronization. It will introduce ISI and degrade the performance. For this reason, the simplified ML estimation method is preferred.

Fractional frequency estimation is performed after symbol timing estimation. Figure 5.13 shows the performance of error standard deviations. Fractional frequency synchronization by using ML estimation and simplified ML estimation schemes are simulated. The added frequency offset for the simulation is 0.2 carrier spacing. The fractional frequency estimator is taken at the estimated symbol start location. The figure shows that performances of these two methods are almost the same, because the detected symbol positions due to the two methods are quite close.

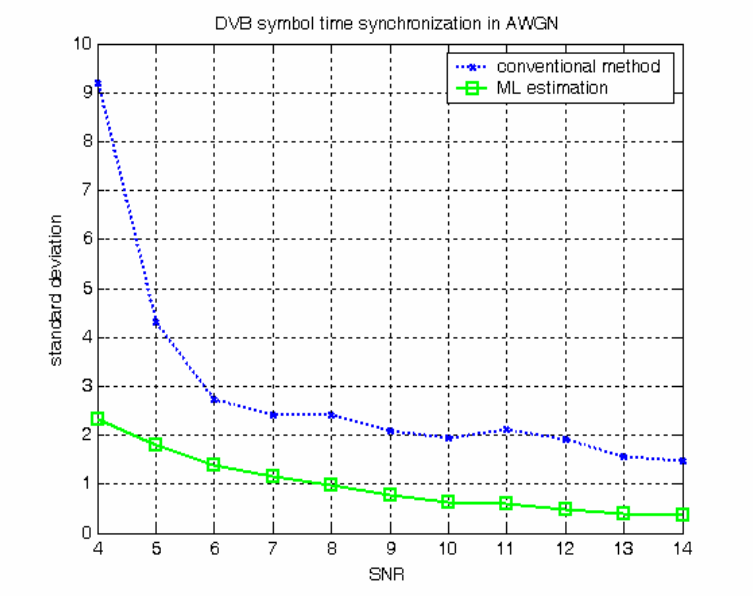

(a)

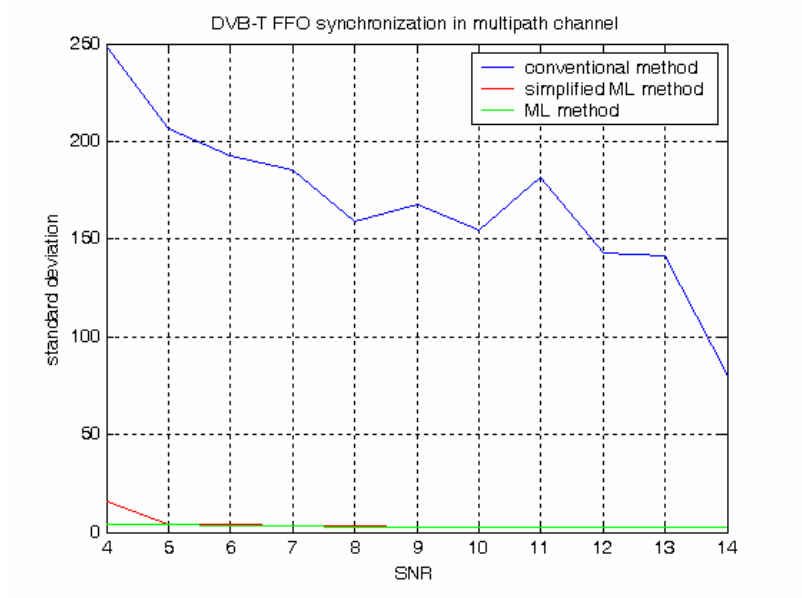

(b)

Figure 5.12 Standard deviation of the time offset estimation errors (a) in AWGN Channel (b) in the assumed multipath channel, 2K-mode DVB-T system.

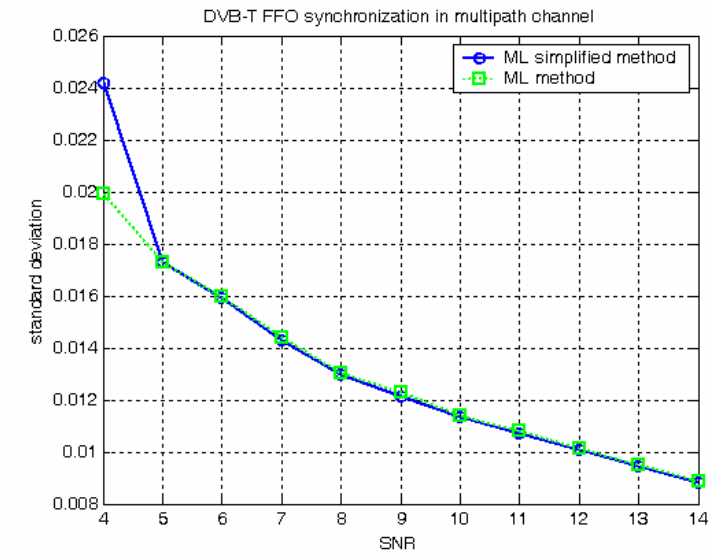

Figure 5.13 Standard deviation of the frequency offset estimation errors in the assumed multipath channel, 2K-mode DVB-T system.

5.2.3 Performance of the Integral Frequency Synchronization

Figure 5.14 shows the failure probability of IFO synchronization in DVB-T 2K mode with our proposed 2 algorithms. It is observed that Algorithm 1 has the better performance than Algorithm 2. We choose Algorithm 1 for other simulations.

Figure 5.15 shows the failure probability of the integer frequency synchronization in DVB-T 2K mode with different Doppler shifts. The assumed frequency offset in our simulation is 2 carrier spacings. The failure probability is about 10^{-3} when SNR is -2dB and there is no Doppler shift. However, the performance worsens when there is a Doppler shift. It is the reason that our algorithm uses the two symbol information to estimate the integral frequency offset. It is sensitive to the variation of the channel conditions. Although 8K mode has long symbol duration that makes it is more sensitive to the variation of the channel conditions, the continual pilots in 8-K mode are more than in 2K mode. Therefore, IFO synchronization performance of 8-K mode is better than that of 2-K mode, as shown in Figure 5.16.

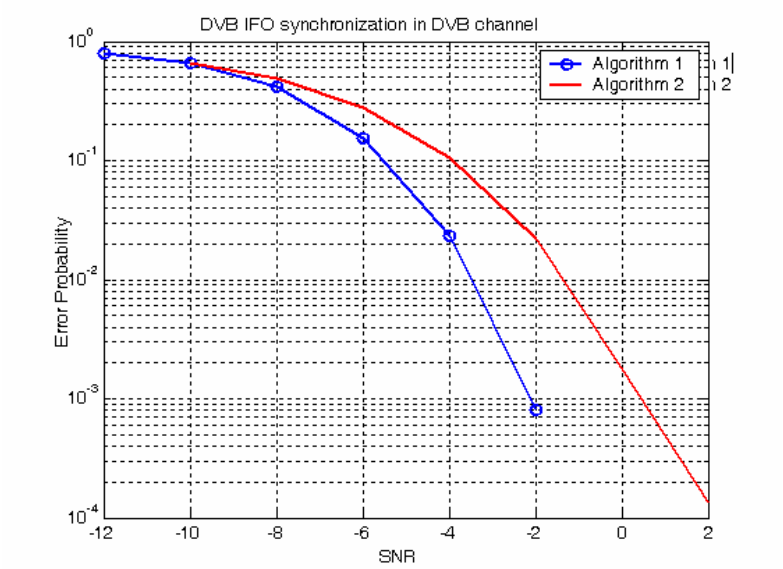

Figure 5.14 Performances of the two proposed integral frequency synchronization algorithms in the assumed multipath channel, 2K-mode DVB-T system.

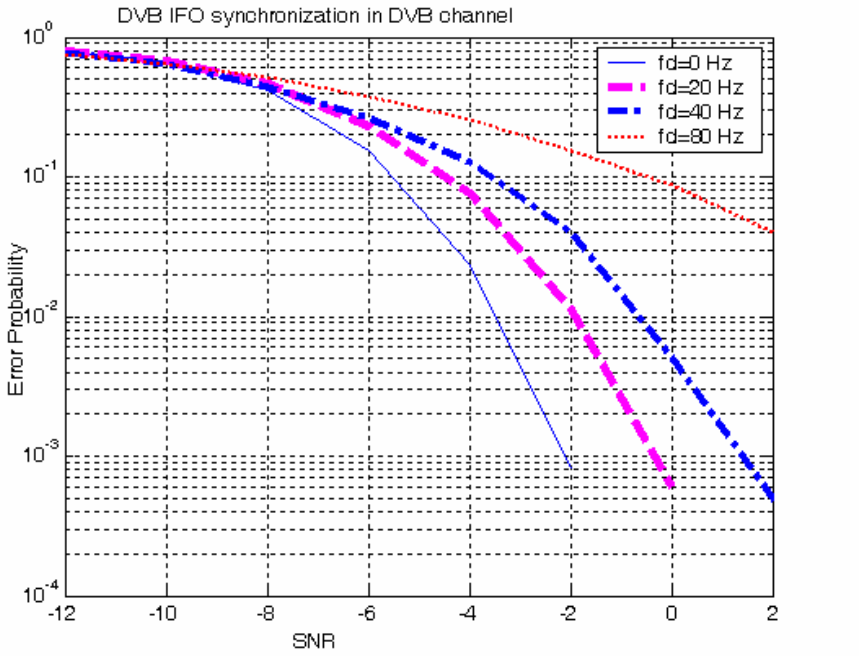

Figure 5.15 Performances of the proposed integral frequency synchronization Algorithm 1 in the assumed multipath channel, 2K-mode DVB-T system.

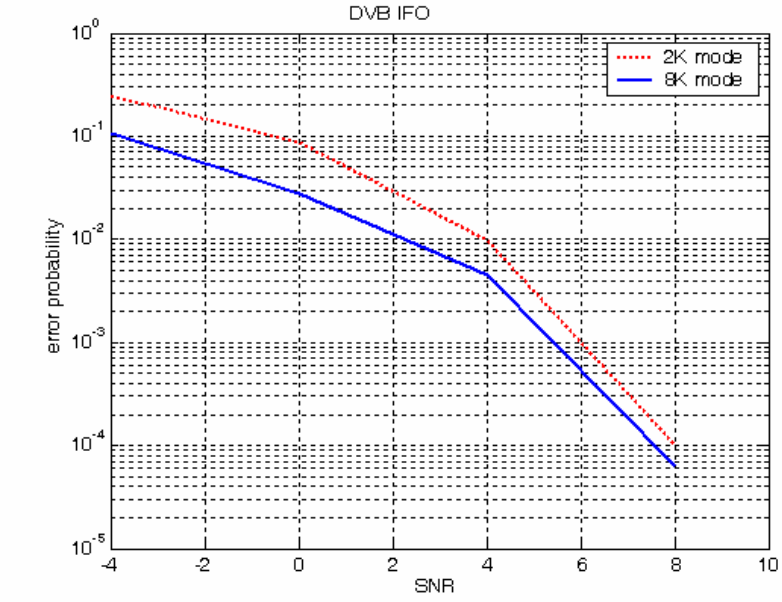

Figure 5.16 Performances of the proposed integral frequency synchronization Algorithm 1 in the assumed multipath channel, fd=90Hz, 2K-mode and 8K-mode DVB-T system.

5.2.4 Performance of the Frame Detection

Here, we use the 17 TPS symbols (1 initialization symbol + 16 synchronization symbol) which are modulated by differential BPSK, for the detection of the frame start. Performance of the frame detection is shown in Figure 5.17. It can be observed from this figure that the algorithm has good performance even in low SNR.

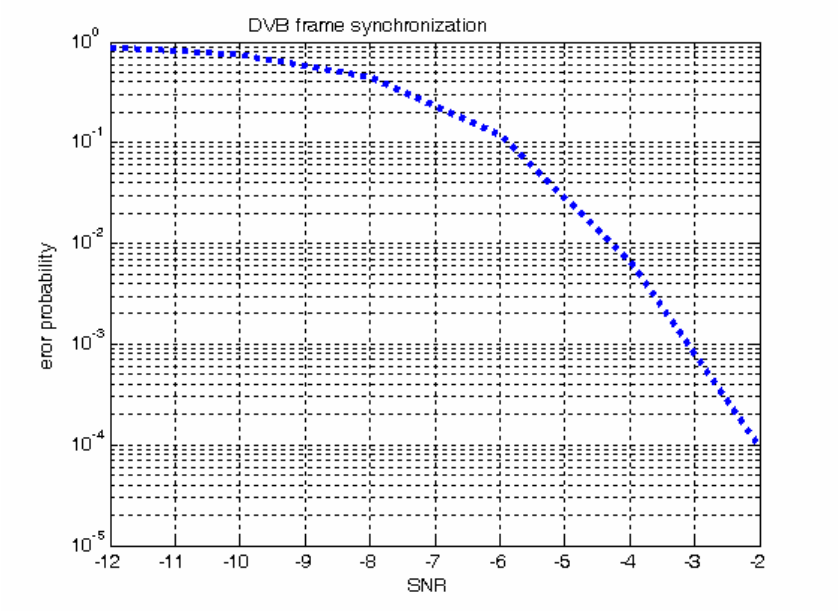

Figure 5.17 Error probability of the adopted frame detection algorithm versus SNR in the assumed multipath channel, 2K-mode DVB-T system.

5.3 IEEE 802.16a

5.3.1 Simulation Parameters and Channel Environments

AWGN channel and multipath channel with SNR from 5dB to 25dB are applied to the simulation. The system parameters are listed in Table 5.5 and the employed ETSI "Vehicular A" multipath channel model is given in Table 5.6. DL synchronization is simulated and analyzed stage by stage as detailed below.

Table5.5: The assumed system parameters of IEEE 802.16a

Center frequency	6 GHz
Bandwidth	20 MHz
Number of carriers	2048
Carrier spacing	11.1607 kHz
Sampling frequency	22.857 MHz
Sampling frequency / Bandwidth	8/7
OFDM symbol time	92.4 μs
Useful time	89.6 μs
Cyclic prefix time	2.8 μs
Cyclic prefix time / Useful time	1/32 (64 samples)

Table 5.6 Characteristics of ETSI 'Vehicular A' channel environment [21]

Tap	**Time delay(μs)**	**Sample number**	**Average Power**	
			(dB)	**(normalized)**
1	0	0	0	0.4850
2	0.31	7	-1	0.3852
3	0.71	16	-9	0.0610
4	1.09	25	-10	0.0485
5	1.73	40	-15	0.0153
6	2.51	57	-20	0.0049

5.3.2 Detection of the Symbol Time

Since IEEE 802.16a DL system is similar to the 2K-mode DVB-T, such as the total number of subcarriers, pilot alignments, and the cyclic prefix length, here we assume a 64-sample cyclic prefix which is the same as in the DVB-T simulation. From Figure 5.17(a) and Figure 5.17(b), it is observed that the conventional method has poor performance due to large channel delay spread. So, we adopt the simplified ML estimation.

In order to avoid ISI, the symbol start location should be selected several samples ahead of the estimated position. From Figure 5.18, 15 samples ahead are reasonable

for SNR higher than 9dB when simplified ML estimation is used.

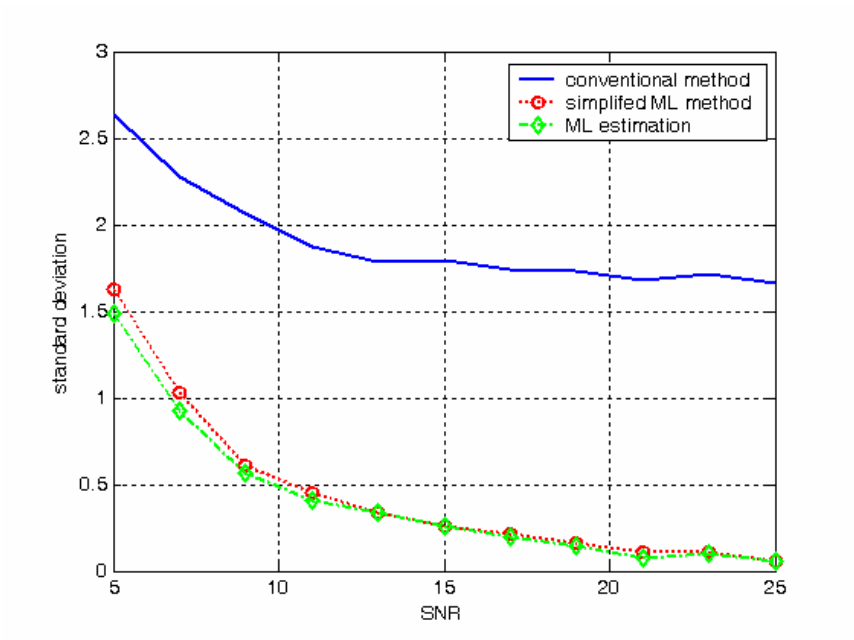

(a)

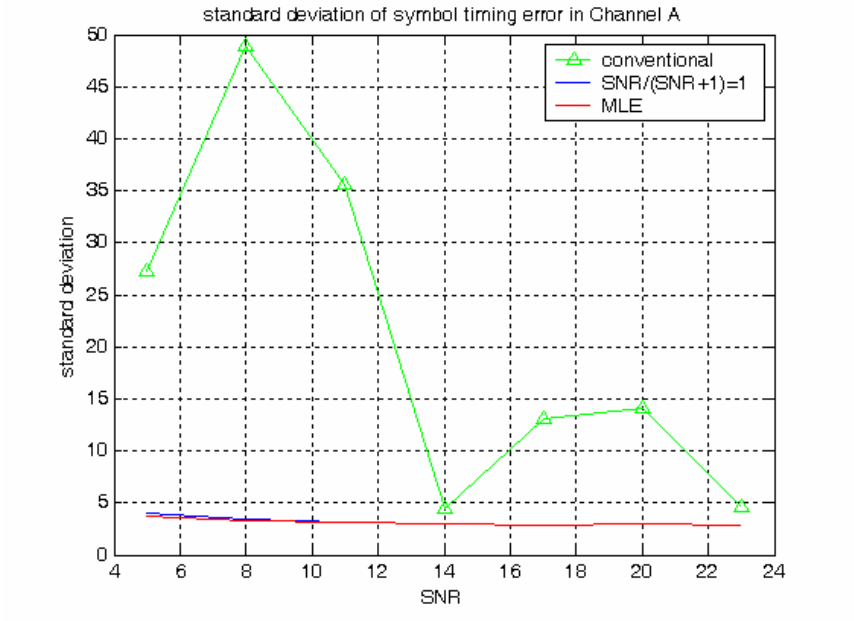

(b)

Figure 5.17 Performances of the time offset estimation methods (a) in AWGN channel; (b) in the assumed multipath channel, IEEE 802.16a DL system.

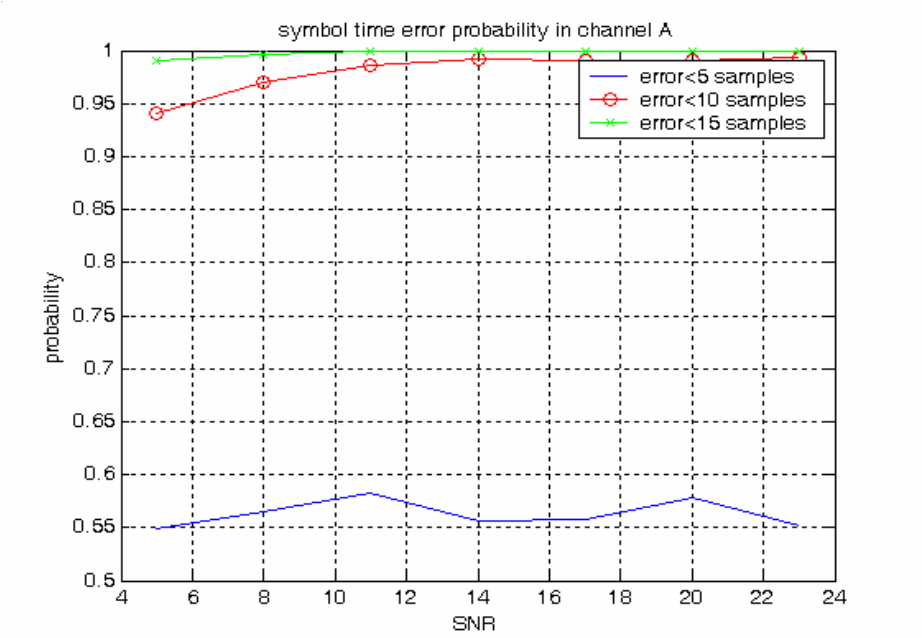

Figure 5.18 Symbol time synchronization error distribution in the assumed multipath channel, IEEE 802.16a DL system.

The assumed fractional frequency offset in this simulation is 0.2 carrier spacings. According to IEEE 802.16a, the center frequency of the SS shall be synchronized to BS with a tolerance of maximum 2% of the carrier spacing. Figure 5.19 shows the percentage of the frequency offset estimates which fall inside the 2% carrier spacing in ETSI channel A. The percentage is viewed as successful probability of frequency synchronization.

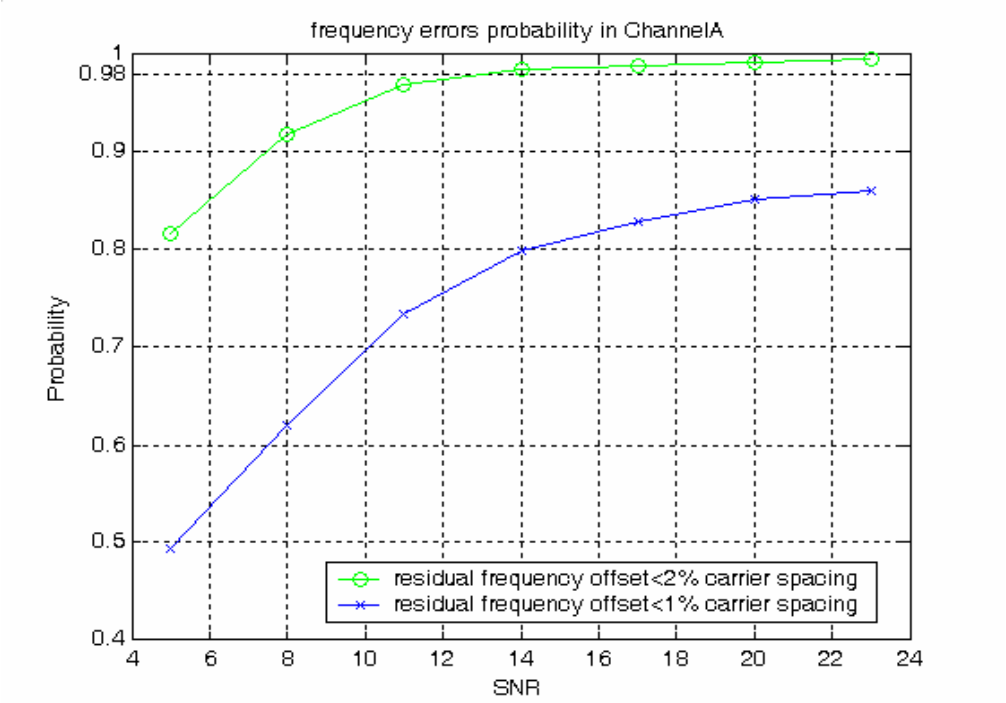

Figure 5.19. Error distribution of the fractional frequency synchronization in the assumed multipath channel, IEEE 802.16a DL system.

5.3.3 Integer Frequency Offset and Frame Synchronization

It is shown in Figure 5.20(a) that the matched filter output $F(g)$ has a peak value equal to 1 at $g=0$ and low values at other positions in noiseless case, if there is no frequency offset and under perfect DL frame synchronization condition. However, mainlobe of $F(g)$ may decrease while the sidelobe increases in AWGN and multipath channels, as shown in Figure 5.20(b). Hence, it degrades the frame lock performance. The value of the metric is always close to zero for any integer g if it is not the first symbol of a DL frame. To exactly detect the coming frame and integer frequency offset, a proper threshold must be set. It is claimed that a frame is coming if the metric $F(\hat{g})$ is larger than the threshold, and $\hat{g}$ is the detected integer frequency offset.

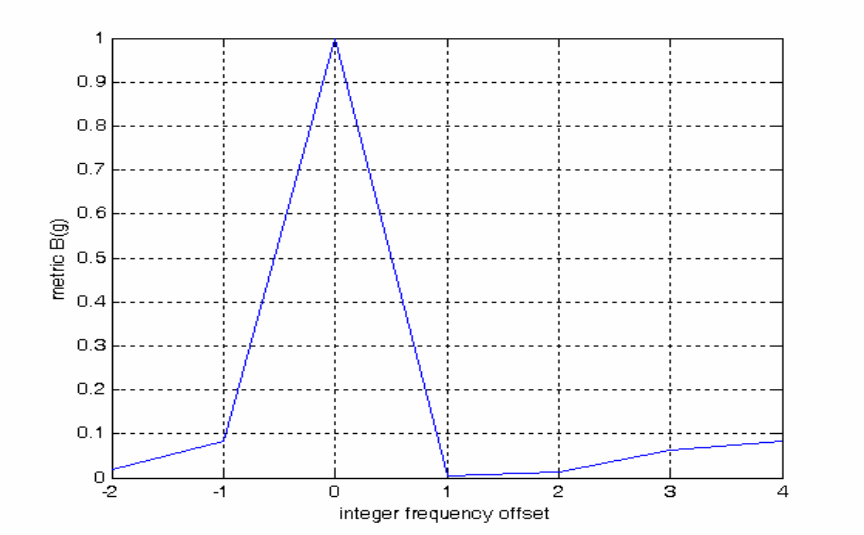

(a)

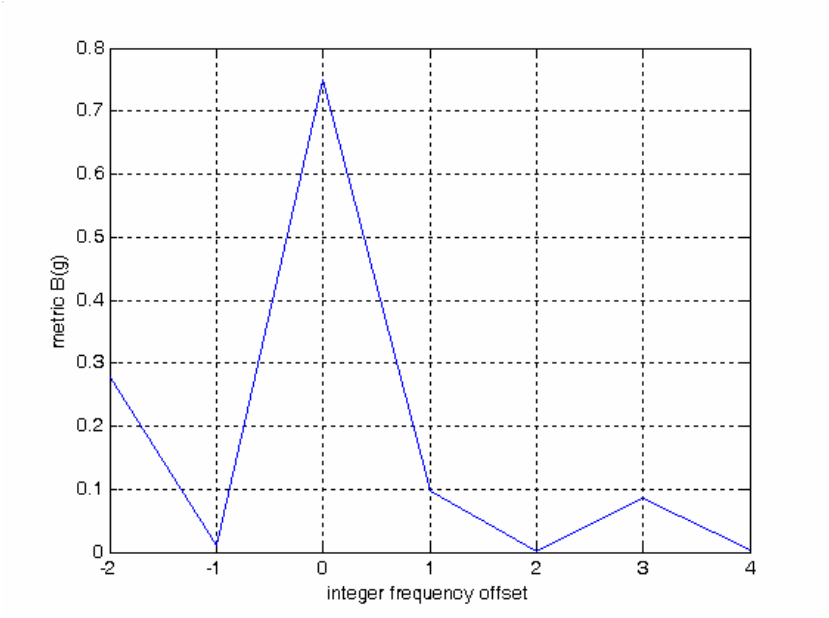

(b)

Figure 5.20. The matched filter output of the first symbol in a frame (a) in noiseless case; (b) in AWGN channel, IEEE 802.16a DL system.

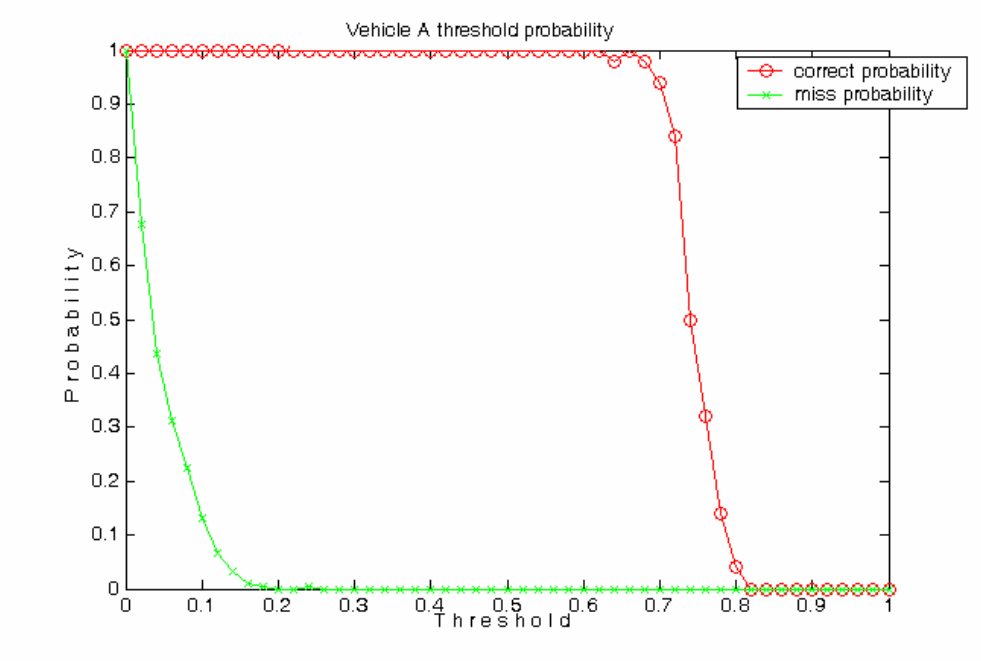

Figure 5.21. Frame synchronization probability versus threshold in multipath channel.

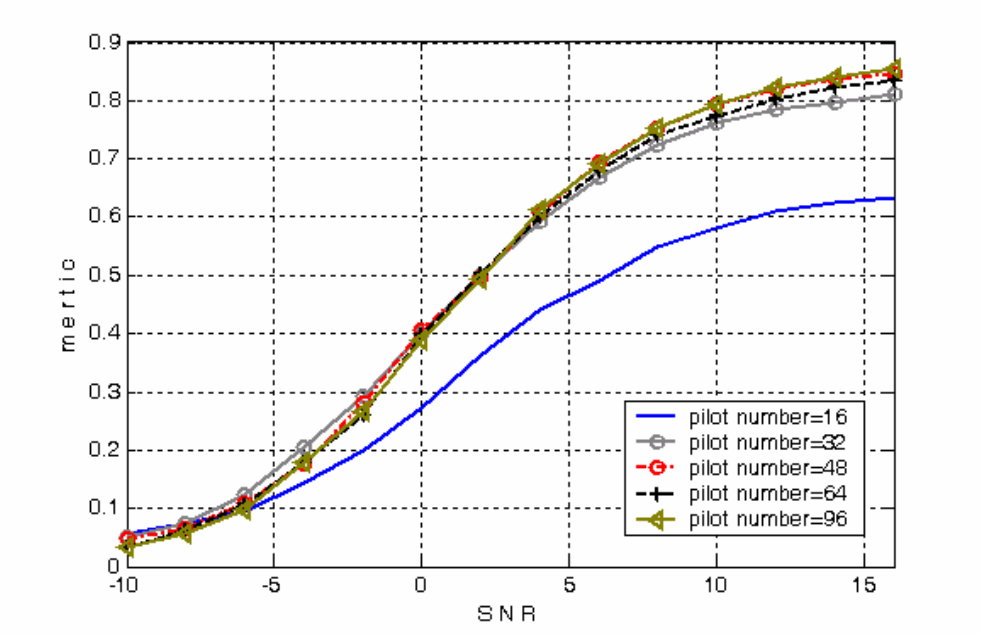

Figure 5.22. Values of IFO and frame synchronization metric vs. pilot number.

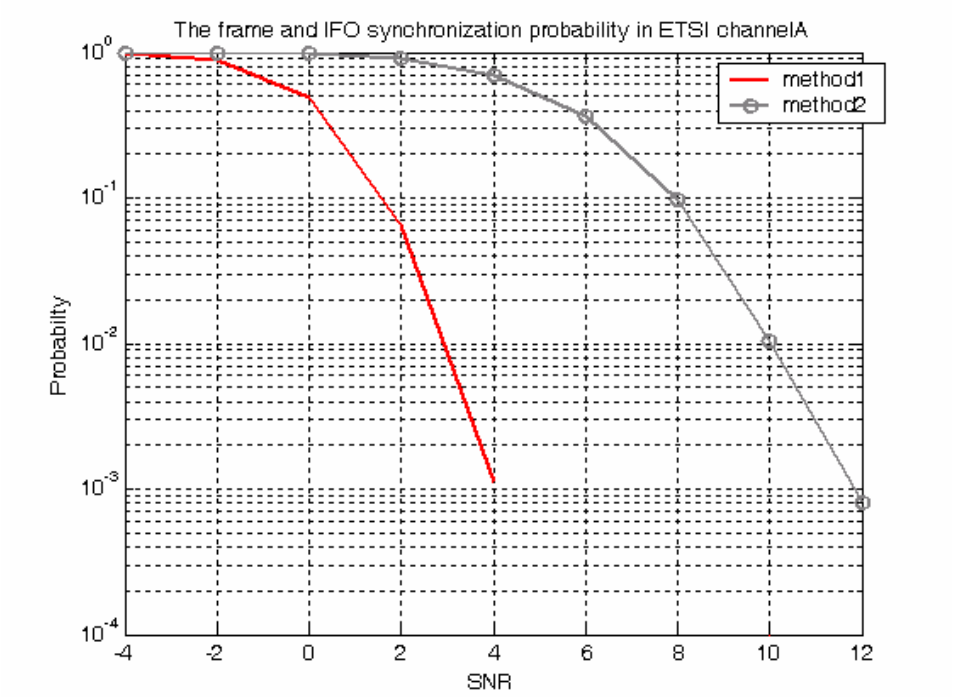

Figure 5.23. Frame and IFO synchronization probability under Channel A, IEEE 802.16a DL system.

The threshold can be well determined by two different probabilities. One is the probability of correct detection of the DL start symbol and the other is the false alarm probability, which means that the detected symbol is not the DL start symbol. The threshold should be chosen that maximizes the probability of correct detection and minimizes the false alarm probability as much as possible. Based on the idea, the threshold is set to 0.4 from the simulation result in Figure 5.21.

IEEE 802.16a standard defines 142 equally-spaced variable-location pilots which can be utilized to do synchronization task for the DL. The trade-off between performance and complexity should be analyzed by computing the IFO and frame synchronization metric as defined in section 4.3.4. The result is shown in Figure 5.22. We can find that the metric converges when the system's pilot numbers are more than 32. Therefore, 32 pilots are chosen for the proposed scheme.

There are two ways in selecting 32 pilots from the 142 variable-location pilots.

Method 1 selects the 32 continuous pilots out of the 142 pilots, while method 2 selects equi-spaced pilots with a spacing of 4 pilots. From Figure 5.23, performance of method 1 is much better than that of method 2. It is understandable that method 1 is more robust against multipath channel than method 2, due to its elimination of the channel phase.

Figure 5.24 shows that the performances of two different cyclic prefix duration in multipath fading channel with $f_d = 333Hz$. Since the symbol which has fixed useful symbol period with a 512-sample cp has a longer symbol duration than the one with a 64-sample cp, it is more sensitive to Doppler shifts.

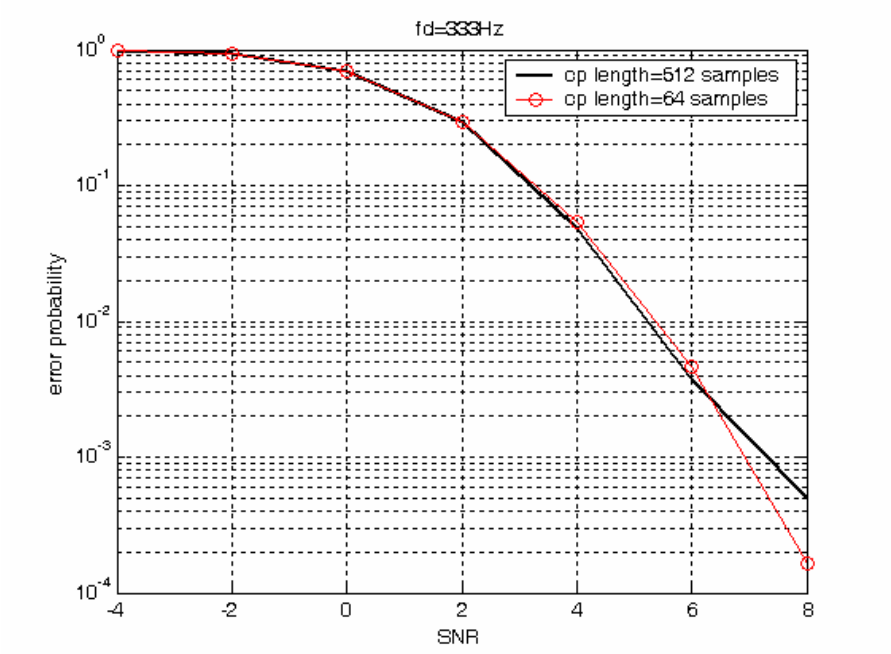

Figure 5.24 Frame and IFO synchronization probabilities of long and short cp's lengths under Channel A, IEEE 802.16a DL system.

5.3.4 System Performance

To evaluate overall performance of the proposed methods for the whole system, the linear interpolation technique is adopted for channel estimation. BER of the proposed system in AWGN channel is shown in Figure 5.25. Perfect synchronization means no timing and frequency synchronization errors. From simulation, the performance loss of the proposed scheme is 2.5 dB at BER = 10^{-5} compared with the perfect synchronization. The BER performance of our method also approaches to the ideal synchronization case in multipath channel, as one can observe in Figure 5.26. Figure 5.27 shows the performance in Rayleigh multipath fading channel. Here we assume $f_d = 133Hz$. The performance loss is due to the Doppler shifts.

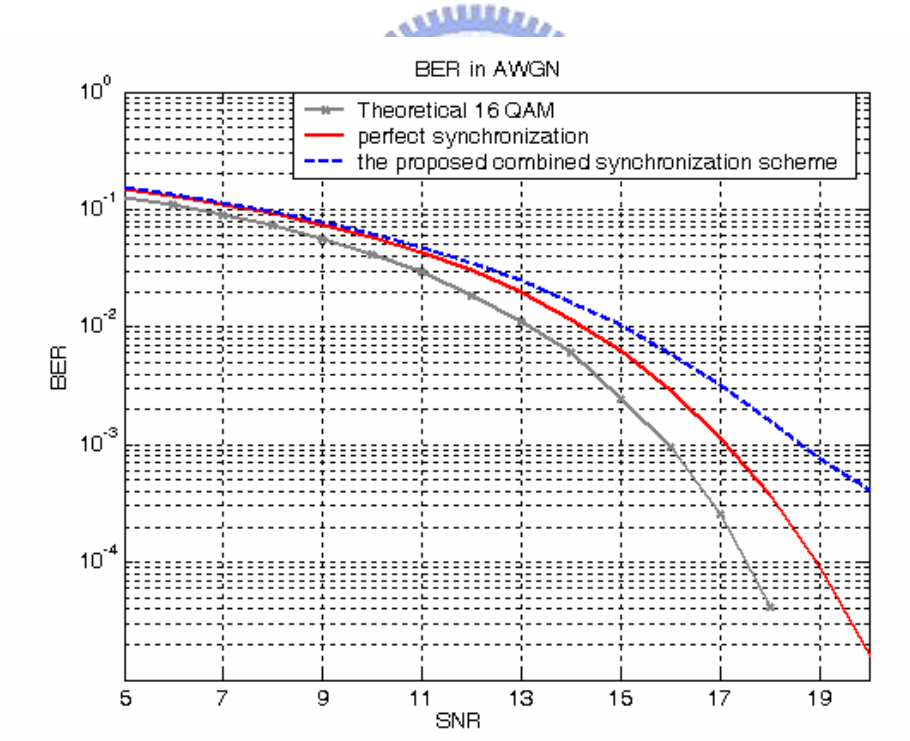

Figure 5.25 BER of the proposed synchronization system in AWGN channel, IEEE 802.16a DL system.

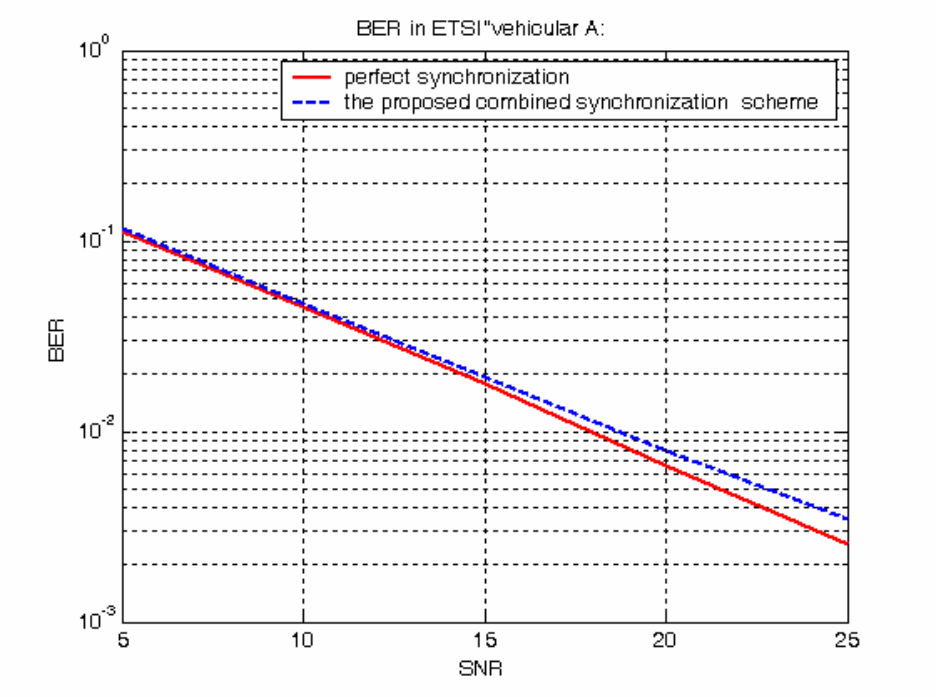

Figure 5.26 BER of the proposed synchronization system in ETSI ”Vehicular A” channel, IEEE 802.16a DL system.

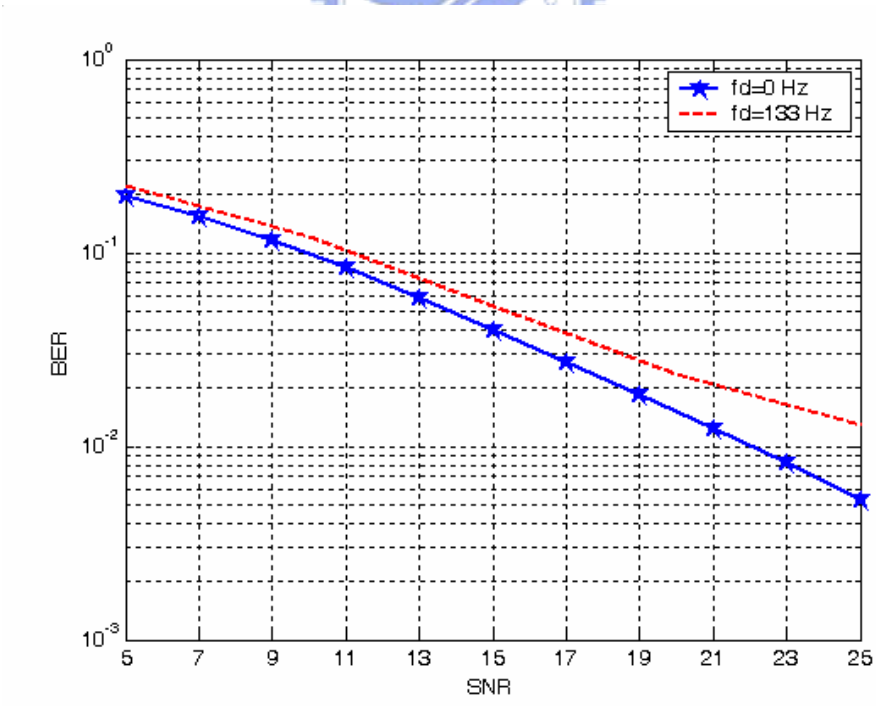

Figure 5.27 BER of the proposed synchronization system in a fading environment, IEEE 802.16a DL system.